Effect of Compressive Creep and Hydrostatic Pressure on Diffusion in NiCr and NiSi Systems

Camille Salsi, Daniel Monceau, Clara Desgranges, Thomas Gheno

Effect of compressive creep and hydrostatic pressure on diffusion in NiCr and NiSi systems

Camille Salsi[a,b*], Daniel Monceau[b], Clara Desgranges[c†] and Thomas Gheno[a]

[a] *DMAS, ONERA, Université Paris Saclay, F-92322 Châtillon, France*
[b] *CIRIMAT, INP-ENSIACET, 4 allée Emile Monso, F-31030 Toulouse, France*
[c] *Safran Tech, rue des jeunes bois, Châteaufort, F-78772 Magny-les-Hameaux, France*

This version of the article has been accepted for publication, after peer review and is subject to Springer Nature's AM terms of use. The Version of Record is available online at: https://doi.org/10.1007/s11661-022-06814-y

Abstract Interdiffusion coefficients were measured in NiSi and NiCr systems from diffusion couples under hydrostatic pressures between 50 and 326 MPa, at 1200 °C. Uniaxial compression creep tests were also carried out on Ni–Cr diffusion couples at 885, 940 and 1000°C with stress values between 0 and 25 MPa, to observe the effect of applied stress on diffusion. A numerical inverse method was elaborated to determine interdiffusion coefficients that takes into account the plastic strain. The comparison of all the diffusion coefficients shows no significant effect of stress for the creep tests and a slight decrease of the interdiffusion coefficients for the hot isostatic pressing (HIP) tests in both systems when the compressive stress increases. This variation is less than twofold, thus the effect is negligible compared to the scatter observed for one diffusion coefficient from different sources of the literature.

Keywords Interdiffusion, creep, NiCr, NiSi, hydrostatic pressure, hot isostatic pressing test, stress, deformation

1 Introduction

High temperature materials are optimized for their mechanical, chemical or physical properties mainly through their chemical composition and microstructure. However, the composition can locally evolve in service due to diffusion. In addition, these materials are often subjected to significant thermomechanical stress that may affect their diffusion properties. It is therefore desirable to evaluate the effect of stress on diffusion if one is to anticipate the behavior of high temperature materials in service conditions.

Several aspects of the effect of stress on diffusion should be distinguished. For example, a stress gradient can act as a driving force for atomic transport, as in the case of rafting of γ/γ' superalloys [1]. Otherwise, stress can directly affect the diffusion coefficient, which is the focus of the present work. The effect of stress and deformation on diffusivity has long been the subject of investigation: among other sources, a review of early theoretical developments and experimental results

*Corresponding author. Email address: camille.salsi at onera.fr
†Present address: Université Paris-Saclay, CEA, SCCME, F-91191, Gif-sur-Yvette

can be found in Ref. [2], a collection of papers on the subject can be found in Ref. [3], while a more recent review can be found in Ref. [4]. This subject has attracted considerable attention in the field of materials for electronics, while less effort has been spent on structure materials such as Ni–base alloys. For example, Nakamura *et al.* [5], studied the effect of high hydrostatic pressure on Ni–Al diffusion couples. They observe a decrease of the interdiffusion coefficient with the pressure in compression. However, their experiments were done under hydrostatic pressures of 3–5 GPa. These stress values are very high and do not necessarily represent the stress magnitude that materials may be exposed to in most of Ni–based alloys applications. Fewer studies address more complex stress states. The effects of different types of elastic loading (hydrostatic, uniaxial and shear stress) on mobility in pure metals was studied by atomistic calculations, e.g., by molecular dynamics in bcc-Fe [6], or by DFT in fcc metals [7]. References [6] and [7] also predict a decrease in mobility under compressive stress, in accordance with linear elasticity theory, with significant amplitude for stress levels in the GPa range. To our knowledge, in Ni–base systems, very few experiments have demonstrated the effect of creep on tracer diffusion [8], and none have addressed the effect of creep on interdiffusion.

This paper examines the effect of viscoplasticity on interdiffusion in the Ni–rich, fcc domain of the binary NiCr system. This was studied using uniaxial compression creep tests conducted on diffusion couples between 885 and 1000 °C, under 0 to 25 MPa. The NiCr system was chosen as it forms the most elementary basis of high temperature Ni–base alloys. Single-phase compositions were used to facilitate the quantitative evaluation of interdiffusion coefficients. The latter were determined with a numerical inverse method that takes into account the strain caused by creep. The absence of precipitation or solid solution strengthening results in low yield stress in these model alloys at the temperatures of interest. Consequently, relative low stress levels were applied in the creep experiments, to avoid excessive strain. In order to distinguish potential contributions of viscoplasticity and elasticity in the creep experiments, Ni–Cr couples of the same composition were subjected to hot isostatic pressing (HIP) experiments. The absence of plastic strain allowed using larger stress levels, up to 326 MPa.

From the standpoint of diffusion properties, the NiCr system is particular in that the intrinsic diffusion coefficients of Cr and Ni have a weak composition dependence, which results in the interdiffusion coefficient having a weak composition dependence as well [9]. Hot isostatic pressing experiments were also conducted on diffusion couples in the NiSi system. Since the diffusivities have a much larger composition dependence, this allows to examine possible element-specific effects of hydrostatic stress, which would affect the composition dependence of the interdiffusion coefficient.

2 Methods

2.1 Materials and experimental method

Diffusion couples were prepared from single-phase alloys with nominal compositions (at. %): Ni, Ni–10Si, Ni–20Cr and Ni–30Cr. Ingots were produced by vacuum induction melting (VIM), homogenized at 1250 °C during 24 h under vacuum, and then cut into 6 x 6 x 3 mm specimens. In order to consider only the diffusion in

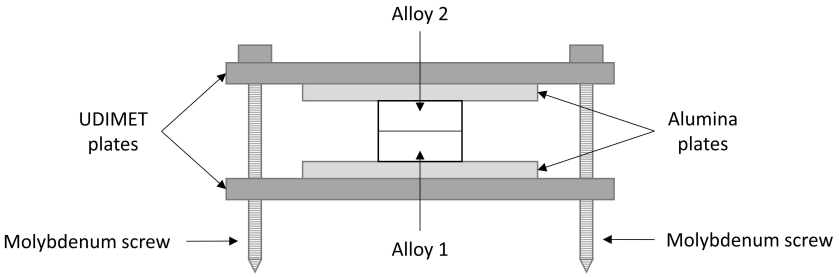

Figure 1: Scheme of the assembling device for the diffusion couples.

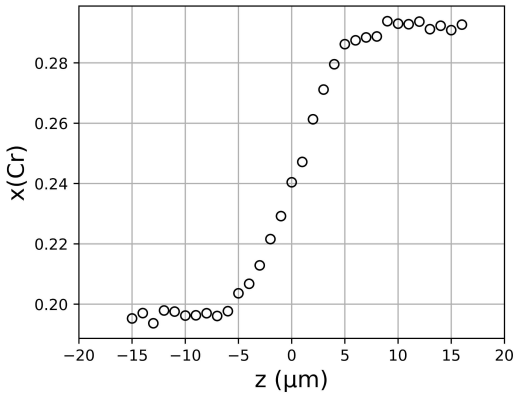

Figure 2: Concentration profile after diffusion couple Ni–20Cr / Ni–30Cr assembly at 1050 °C during 1 hour, where x_{Cr} corresponds to the atomic fraction of chromium.

volume, and not the diffusion at the grain boundaries, the time and temperature of the homogenization treatment have been chosen to obtain alloys with millimetric grain size. To form a diffusion couple, one face of each alloy to be assembled was polished with SiC paper down to a P4000 grade. Particles of $Gd_2Zr_2O_7$ of average diameter 1 µm were deposited on one alloy, to serve as inert markers. The alloys were then placed between two plates of Ni–based superalloy (UDIMET 720) held together with molybdenum screws and nuts (Figure 1), and the assembly was heat treated 1 h at 1050 °C under vacuum. The alloys to be assembled have a much higher coefficient of thermal expansion than the molybdenum screws. The stress resulting from this difference, about 50 MPa in the conditions of interest, causes the alloys to bond. In addition, the conditions of the assembly treatment were chosen so that the diffusion distance (due to the assembly) is negligible compared to the diffusion distance of the test. Concentration profiles in Ni–Cr diffusion couples were measured after assembly to verify the latter condition. As shown on Figure 2, the diffusion distance is about 10 µm, whereas after diffusion in the conditions of interest it is between 100 and 200 µm.

After bonding, the couples were removed from the assembling device and subjected to diffusion heat treatments.

Uniaxial compression creep tests were carried out on Ni–Cr diffusion couples at constant temperature (885 – 1000 °C), controlled by a type S thermocouple, in air under constant compressive stress. To select stress values, a compression test was

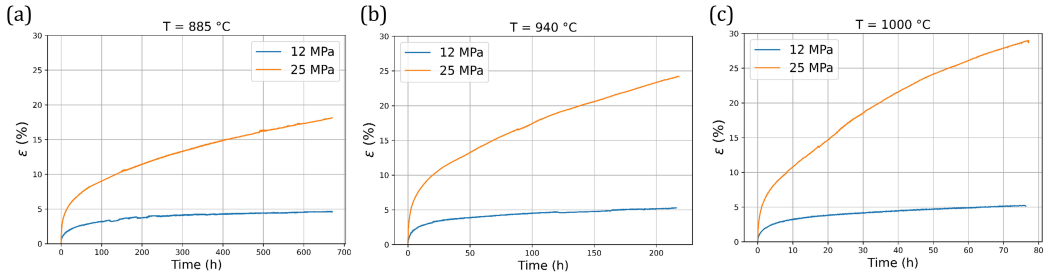

Figure 3: Strain vs. time for compression creep tests carried out on Ni–20Cr / Ni–30Cr diffusion couples at (a) 885 °C, (b) 940 °C and (c) 1000 °C in air during 670, 216 and 77 hours respectively.

Table 1: Conditions for creep and HIP tests on Ni–Cr and Ni–Si diffusion couples. Composition is given in at. %.

Mechanical test	Diffusion couple	Temperature (°C)	Time (h)	Stress (MPa)	Atmosphere
Creep	Ni–20Cr / Ni–30Cr	885 940 1000	670 216 77	0, 12, 25	Laboratory air
HIP	Ni–20Cr / Ni–30Cr Ni / Ni–10Si	1200	5	50, 100, 326	Argon

carried out on Ni–30Cr alloy at 1000 °C and the yield strength was measured. The latter was about 37 MPa, thus the applied stress values were in the range of 0 to 25 MPa. The sample was oriented so that the stress direction is perpendicular to the interface. The heating rate was about 5°C/min and the load was applied and removed at high temperature. During creep test, the strain was measured by the extensometer. Figure 3 illustrates the strain as a function of time. It shows a plastic strain of about 5 % for 12 MPa and between 18 and 29 % for 25 MPa. The secondary creep stage is not exceeded. Furthermore, given the high temperature ($T > 0.6\ T_f$) and the low stress level ($\sigma <$ yield strength), deformation most likely occurs by the diffusion of vacancies (diffusion creep).

Hot pressing tests were carried out on Ni–Cr and Ni–Si diffusion couples during 5 h under pressure (50–326 MPa) at 1200 °C with heating and cooling rates of 12 °C/min. The chamber was pressurized during the temperature rise. Table I summarizes creep and HIP test conditions.

After the diffusion treatment, cross sections were analyzed by scanning electron microscopy (SEM) in a FEG-SEM Zeiss Merlin. Concentration profiles were measured by energy dispersive X-ray (EDX) using a quantification procedure with pure metals as standards (SAMx acquisition software). These concentration profiles were then used to determine interdiffusion coefficient by a numerical inverse method, presented in the following part.

Repeatability tests were carried out to determine the uncertainty on the diffusion coefficient. For that, the same experiment was done three times and for each

sample two concentration profiles were measured by SEM. This method provides a measurement random error about 9.3 % on the interdiffusion coefficient.

2.2 Determination of interdiffusion coefficient in a binary system

The estimation of interdiffusion coefficient can be performed either using an analytical direct method or a numerical inverse method. For a binary system, the main analytical methods are the Boltzmann-Matano and Sauer-Freise methods [10]. The Boltzmann-Matano method gives as accurate results as the Sauer-Freise method but it requires determining the Matano plane, which can be challenging, especially if experimental concentration profiles are noisy. In contrast, the Sauer-Freise method does not rely on the Matano plane. However, both methods result in inaccurate values of diffusion coefficients at the terminal concentrations. On the other hand, these problems are not encountered with numerical inverse methods. By imposing the composition dependence of the diffusion coefficient, these methods also reduce artifacts associated with noise in the concentration profiles. Numerical inverse methods consist in fitting parameters which define the composition dependence of the interdiffusion coefficient by minimizing the difference between experimental and simulated concentration profiles [11]. The simulated profiles are obtained by solving the diffusion equation, which corresponds to the combination of the Fick's law (1) and the continuity equation (2) [12].

$$J_{\mathrm{A}} = -\tilde{D}_{\mathrm{AB}} \frac{\partial c_{\mathrm{A}}}{\partial z} \tag{1}$$

$$\frac{\partial c_{\mathrm{A}}}{\partial t} = -\frac{\partial J_{\mathrm{A}}}{\partial z} \tag{2}$$

In Eqs. (1) and (2), J_{A} and c_{A} refer to the flux in the laboratory frame of reference (see Appendix) and the concentration of species A, respectively, and $\tilde{D}_{\mathrm{AB}}$ to the composition-dependent interdiffusion coefficient for a binary system AB. In this work, the composition dependence of the interdiffusion coefficient is described by a polynomial function, where a_i are the fitting parameters:

$$\tilde{D}_{\mathrm{AB}} = \sum_{i=0}^{n} a_i * c_{\mathrm{A}}^i \tag{3}$$

The diffusion equations are solved by the finite difference method, implemented in a Python script. The optimization of the parameters describing the composition dependence of the interdiffusion coefficient is performed with the *least_squares* function (Levenberg-Marquardt algorithm) from the *Scipy* library [13] and using the *Numpy* library [14]. The minimization consists in determining the difference between the experimental and a simulated concentration profile by calculating a residual. Figure 4 explains schematically the detailed process of the optimization.

To estimate the order of the polynomial of the Eq. (3) best adapted to the experimental results, several tests were performed. Figure 5 illustrates the evolution of the residual on the concentration profile with the polynomial order n (up to 5) for the composition dependence of the diffusion coefficient. For NiCr system the residual stays nearly constant for all orders, while for NiSi the residual is constant only for an order greater than or equal to 1. Therefore, we chose a polynomial of order 0 (constant interdiffusion coefficient) in the NiCr system, and a polynomial

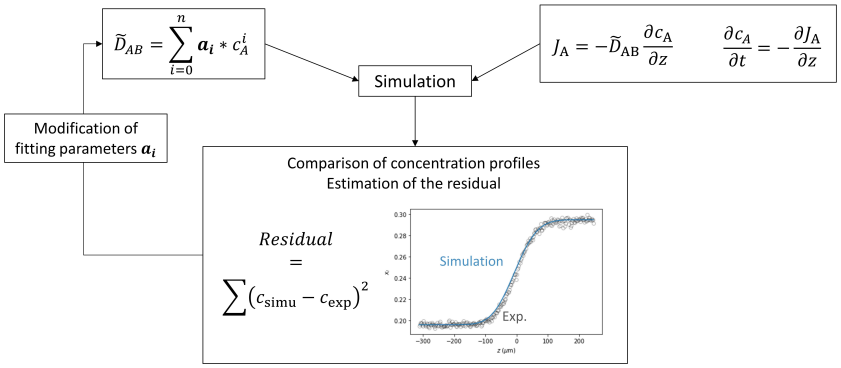

Figure 4: Diagram explaining the running of the python code for determining interdiffusion coefficients by a numerical inverse method. The Levenberg-Marquardt algorithm (from the function "least_squares" of the Scipy library [13]) is used for the minimization between experimental and simulated profiles.

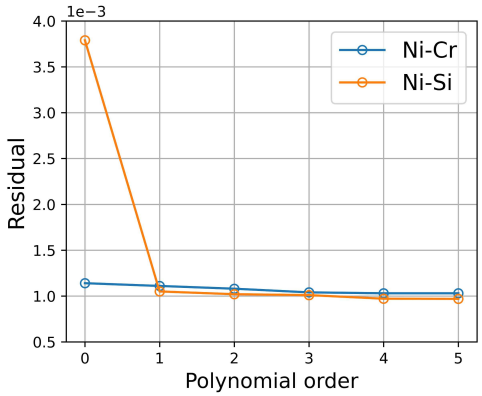

Figure 5: Residual on concentration profiles as a function of polynomial order of Eq. (3) for NiCr and NiSi systems

of order 1 (linear variation of the interdiffusion coefficient with the composition) in the NiSi system. These observations are consistent with the stress-free diffusivity data available in these systems. Calculations made with data from Du and Schuster [15,16] indicate that, at the temperatures of interest, $\tilde{D}_{\mathrm{NiCr}}$ is nearly constant in the composition range investigated, while $\tilde{D}_{\mathrm{NiSi}}$ varies significantly with Si composition. The composition range investigated (0–10 at. % Si) is narrow, and in this range the variations of $\tilde{D}_{\mathrm{NiSi}}$ can be described as linear.

Since diffusion may be affected by the applied stress and the deformation, this method for measuring interdiffusion coefficients has to be adapted. The flux of species A in a binary alloy AB subjected to composition and stress gradients is written as [12]:

$$J_{\mathrm{A}} = -\tilde{D}_{\mathrm{AB}}\,(P)\,\frac{\partial c_{\mathrm{A}}}{\partial z} - \frac{\tilde{D}_{\mathrm{AB}}(P)}{k_{\mathrm{B}}T}\frac{\mathrm{d}U}{\mathrm{d}z} \tag{4}$$

with $\tilde{D}_{\mathrm{AB}}(P)$ the pressure-dependent interdiffusion diffusion coefficient, k_{B} the Boltzmann constant, T the temperature and U the elastic interaction energy in the stress

```
# initialize
dz_init = z_max/nz

# time loop
for n in range(nt):
    dzⁿ = dz_init * (1 - εⁿ)    # resize mesh
    Dⁿ = Σⱼ(aⱼ*Cʲ)
# spatial loop
    for i in range(nz):
       Jⁿᵢ₊₁ = - Dⁿ * [Cⁿᵢ₊₁ - Cⁿᵢ]/dzⁿ
       Cⁿ⁺¹ᵢ = Cⁿᵢ – dt * [Jⁿᵢ₊₁ - Jⁿᵢ]/dzⁿ
```

Figure 6: Pseudo-code of the diffusion solver, in which the red highlighted line represents the expression to add to take into account the deformation with time ε^n during creep tests. Indices n and i refer to the time and space, respectively.

field. In the first term of Eq. (4), the diffusion coefficient will vary because of the hydrostatic contribution of stress, while the second term represents the flux induced by the stress gradient. In an uniaxial compression creep test (if contact friction between the traverses and the specimen is neglected), there is no stress gradient and only the first term of Eq. (4) remains, i.e., the usual flux expression, Eq. (1), can be considered, with a pressure-dependent interdiffusion coefficient. This also applies to the HIP tests, which generate no stress gradient.

In the case of the creep experiments, the dimensions of the specimens change over time, which affects the measured concentration profiles. As shown in the Appendix, with two simplifying assumptions, the 3D problem of creep-interdiffusion reduces to a 1D problem, with all deformation-related effects gathered into an apparent interdiffusion coefficient. The assumptions are the following:
(i) creep can be described as a convective form of transport, and
(ii) the diffusivity and mechanical properties are uniform throughout the couple.

The time evolution of the composition can then be computed by solving the diffusion equation in a frame of reference fixed to the sample that strains with time. The hypothesis of uniform mechanical properties implies that the strain in the load direction (z axis) is equally distributed over the diffusion couple. Strain is interpolated from the experimental data (Figure 3) and the strain value calculated at each time step is converted into a variation of the space step, as shown in Figure 6. Taking into account the strain is important as a strain of about 30 % can lead to an apparent variation of the interdiffusion coefficient of about 20 % if the strain is not taken into account.

3 Results

Cross sections of the diffusion couples were observed by SEM and show that no pore were formed due to the Kirkendall effect for Ni–Cr and Ni–Si systems. Concentration profiles were measured and the origin of the distance axis (z = 0) was placed at the location of the inert markers, i.e., at the Kirkendall plane. The position of the Matano plane was determined from the concentration profiles, according to the classical method [17], which then provided the Kirkendall shift. For the Ni–Cr

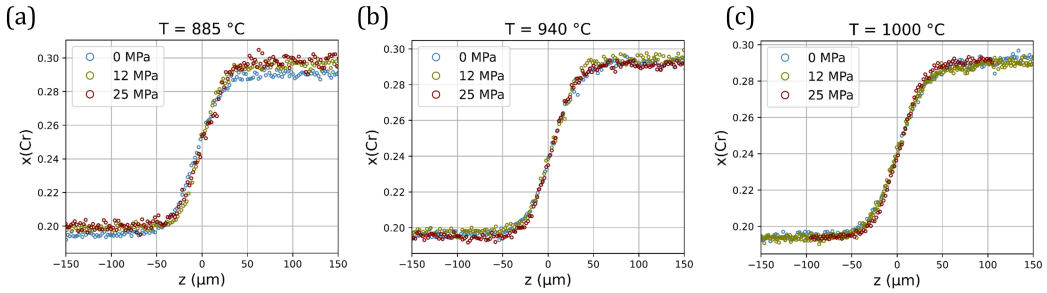

Figure 7: Concentration profiles of Ni–20Cr / Ni–30Cr diffusion couples heat treated at (a) 885 °C, (b) 940 °C and (c) 1000 °C during 670, 216 and 77 hours, respectively, with 0, 12 and 25 MPa (compression creep tests)

diffusion couples, regardless of the temperature the Kirkendall shift was found to be less than 1 µm. In the Ni–Si couples, the measured values were slightly larger but also smaller than 1 µm.

On Figure 7, concentration profiles measured in the NiCr couple after compression creep tests with different stress levels are superposed for comparison at each temperature. We can see that the concentration profiles are almost identical for all stress values at each temperature. The profiles were used to evaluate the interdiffusion coefficients using the numerical inverse method described previously.

Figure 8 shows the evolution of the interdiffusion coefficient with temperature for all stress values. Without stress, the Ni–Cr interdiffusion coefficient is in agreement with literature data. Using diffusion data from Jönsson [18] and thermodynamic data from Lee [19], the interdiffusion coefficient is calculated to be fairly constant between 20 and 30 at.% Cr, with an average value of 7.5 x 10^{-16} m^2/s at 1000 °C. In comparison, the estimated diffusion coefficient at 1000 °C in this work is 1.5 x 10^{-15} m^2/s. Table II compares the values of the constant Ni–Cr interdiffusion coefficient determined in this work and that determined using data of Jönsson and Lee for all temperatures.

On Figure 8, a small variation of the interdiffusion coefficient with stress is observed at 1000 °C: an increase of the stress from atmospheric pressure to 25 MPa results in a decrease in the interdiffusion coefficient of about 76 %. However, the data at 940 and 885 °C do not follow any consistent trend. At 885 °C, the point at 12 MPa is far from the others, probably due to an experimental error. Overall, the small variations observed here may not be distinguished from experimental dispersion with confidence: no significant effect of stress is found in the conditions of these experiments.

Figure 9 shows the concentration profiles and the evolution of the interdiffusion coefficient with pressure in NiCr after HIP tests at 1200 °C. A slight decrease in the interdiffusion coefficient with pressure is observed.

For the NiSi system, Figure 10 presents the experimental concentration profiles for each tests and the interdiffusion coefficients, which depend linearly on the composition. The concentration profiles are very close to each other, but there are visible differences on the diffusion coefficients. As for the previous tests the decrease observed with pressure is small: for an increasing pressure ratio around 6.5 (between 50 and 326 MPa), a decrease of up to 66 % on the interdiffusion coefficient is ob-

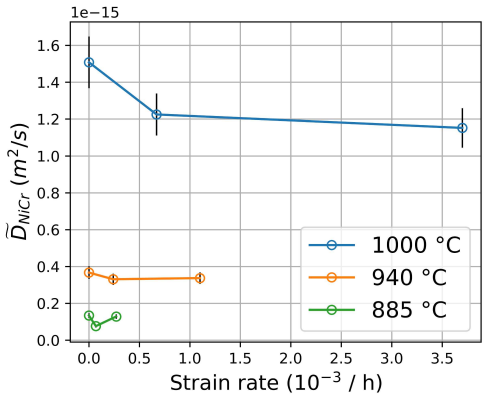

Figure 8: Evolution of the Ni–Cr interdiffusion coefficient with creep strain rate at 885, 904 and 1000 °C. Error bars represents the measurement random error determined from the repeatability tests.

Table 2: Comparison of the constant Ni–Cr interdiffusion coefficient determined in this work and using data from the literature.

Temperature (°C)	Ni–Cr interdiffusion coefficient (m^2/s)	
	using data from Jönsson [18] and Lee [19]	this work
885	5.5 x 10^{-17}	1.3 x 10^{-16}
940	2.1 x 10^{-16}	3.7 x 10^{-16}
1000	7.5 x 10^{-16}	1.5 x 10^{-15}

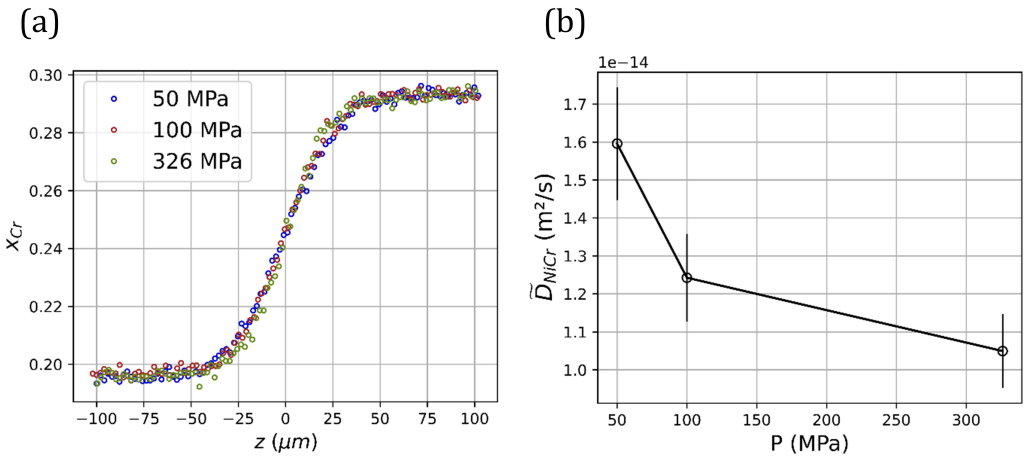

Figure 9: (a) Concentration profiles and (b) evolution of the Ni–Cr interdiffusion coefficient with pressure for hot isostatic pressing tests on Ni–Cr diffusion couples at 1200 °C during 5 hours. Error bars represents the measurement random error determined from the repeatability tests.

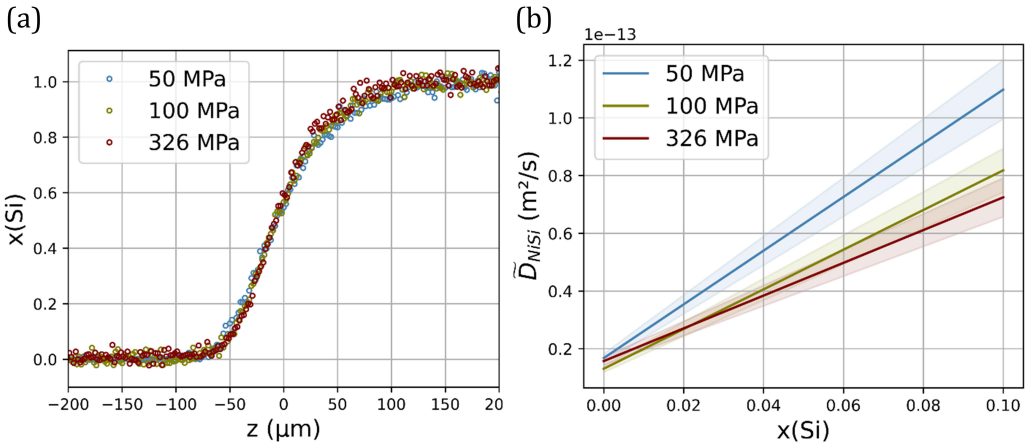

Figure 10: (a) Normalized concentration profiles and (b) evolution of Ni–Si interdiffusion coefficient with Si composition at several pressures after hot isostatic pressing tests on Ni–Si diffusion couples at 1200 °C during 5 hours. The colored background areas represent the measurement random error determined from the repeatability tests.

served, that is greater than for the variation observed for the creep test at 1000 °C. Finally, one can notice that the pressure effect varies with the composition: there is almost no effect of pressure in pure nickel and a significant effect can be observed in Ni–10Si.

4 Discussion

In a binary AB system, the interdiffusion coefficient is related to the tracer diffusion coefficients via the Darken relation:

$$\tilde{D}_{\mathrm{AB}} = (c_{\mathrm{A}} D^*_{\mathrm{B}} + c_{\mathrm{B}} D^*_{\mathrm{A}})\phi \tag{5}$$

where D^*_i is the tracer diffusion coefficient of species i, and ϕ is the thermodynamic factor, defined by

$$\phi = \frac{c_{\mathrm{A}}}{RT}\frac{\partial \mu_{\mathrm{A}}}{\partial x_{\mathrm{A}}} \tag{6}$$

In Eq. (6), μ_{A} is the chemical potential of A, R is the ideal gas constant and T the temperature. The thermodynamic factor is not expected to vary significantly with the pressure. The discussion therefore focuses on the tracer diffusion coefficients. In a cubic crystal, the latter may be written in the general form

$$D^*_i = g f a^2 \nu_0 \exp\left(-\frac{\Delta G}{RT}\right) \tag{7}$$

where g and f are geometry and correlation factors, respectively, a is the lattice parameter, ν_0 is the jump attempt frequency, and ΔG is the Gibbs free energy of diffusion. All terms in Eq. (7) may be affected by stress and deformation, to extents that depend on the diffusion mechanism and the loading conditions [2]. The discussion first addresses the case of elastic deformation, before turning to plastic deformation.

The effect of hydrostatic pressure on diffusivity is mainly due to the pressure dependence of ΔG [4],

$$\Delta G = \Delta U + P\Delta V - T\Delta S \tag{8}$$

where ΔU is the activation energy, ΔV the activation volume and ΔS the entropy of activation. Diffusion in metals occurs by a vacancy mechanism; ΔG may then be split into vacancy formation and migration energies, $\Delta G = G^F + G^M$, where the pressure dependence of each term follows Eq. (8). It follows that the tracer diffusivity can be written

$$D_i^* = gfa^2\, c_{\mathrm{V}}^{\mathrm{eq}}(T,P)\ \Gamma(T,P) \tag{9}$$

where the equilibrium vacancy concentration is

$$c_{\mathrm{V}}^{\mathrm{eq}}(T,P) = \exp\left(-\frac{U^F + PV^F - TS^F}{RT}\right) \tag{10}$$

and $\Gamma(T,P)$ is defined by

$$\Gamma(T,P) = \nu_0 \exp\left(-\frac{U^M + PV^M - TS^M}{RT}\right) \tag{11}$$

Experimental data have shown that diffusion in fcc metals occurs by a monovacancy mechanism at the temperatures of interest, with activation volumes that range between 0.7Ω and 0.9Ω (Ω is the molar volume) ([4,12]). These values are consistent with recent DFT results for diffusion in pure fcc Ni [7]: $V^F = 0.61\Omega$, $V^M = 0.15\Omega$, which yield $\Delta V = 0.76\Omega$. Using these values, it is possible to evaluate the ratio of two tracer diffusion coefficients at two different pressures. When the pressure increases from 50 to 326 MPa, we expect D^* to be divided by 1.2 at 1200 °C. The present experimental results are consistent with this expected variation: in the HIP tests, a ratio about 1.5 is obtained between the interdiffusion coefficients measured at 326 and 50 MPa.

Non-hydrostatic loading conditions (uniaxial or pure shear for instance) introduce a loss of crystal symmetry, and the terms of Eq. (9) become orientation-dependent. This has been studied by analytical methods [20,21] and first-principle calculations [6,7]. However, the phenomena described previously are caused exclusively by elastic deformation and the most significant feature of diffusion under uniaxial loading, as in the present work, is related to the occurrence of viscoplastic deformation. The latter may be due to vacancy diffusion or to dislocation glide or climb, which corresponds respectively to diffusion creep or dislocation creep. As mentioned in Section 2.1, in the present work viscoplastic deformation is due to diffusion creep. Since the two creep mechanisms might have a different impact on diffusion, it is relevant to study their effects separately. In the following section, we will discuss the effect of dislocation creep observed in the literature and compare it with the results of this work, in order to deduce the impact of each mechanism on diffusion. No direct comparison of the present results can be made with experimental data from the literature, as no other study on the effect of diffusion creep on interdiffusion could be found.

According to the early review by Girifalco and Grimes [2], in the conditions typical of dynamic strain, the main contribution of deformation to diffusivity is due

to the vacancy concentration, which is believed to increase and depart significantly from its equilibrium value as a result of dislocation climb. Note that the vacancy concentration, and therefore the tracer diffusivity, are expected to increase whether the applied load is in tension or compression. At steady-state, the diffusivity variation is expected to vary linearly with the strain rate [2]:

$$\frac{D_s^*}{D_u^*} = 1 + \frac{K_1 \dot{\varepsilon}}{K_2 c_V^u}, \tag{12}$$

where the indices s and u refer to strained and unstrained quantities, respectively, $\dot{\varepsilon}$ is the strain rate, K_1 reflects the vacancy production rate due to the plastic strain, and K_2 reflects the strength of other vacancy sources/sinks (dislocation jogs, grain boundaries, precipitates, pores). The linear dependence represented by Eq. (12) was observed experimentally: in Ref. [22], the self-diffusivity of bcc Fe was measured using the tracer method during uniaxial compression, and was found to increase linearly with the strain rate. The variation was described by

$$\frac{D_s^*}{D_u^*} = 1 + 50\dot{\varepsilon} \tag{13}$$

with $\dot{\varepsilon}$ in h^{-1}. The strain rates measured in the present creep experiments were in the range 7 x 10^{-5}– 3.70 x 10^{-3} h^{-1}, which would not produce significant diffusivity variations if the same relationship was obeyed.

Nevertheless, the slight decrease of the interdiffusion coefficient measured in the creep tests at 1000 °C (Figure 8) is at variance with the above formalism [2], since the latter anticipates an increase of the diffusion coefficient under dynamic strain, even in compression. Therefore, the decrease observed at 1000 °C in this study is not due to the effect of viscoplastic deformation introduced by Buffington and Cohen [22]. Furthermore, if we refer to the first-principles results of Refs [6,7], given the stress levels involved in the present creep experiments (12 and 25 MPa), neither the hydrostatic nor the deviatoric stress is expected to significantly affect the diffusivity. Factors other than vacancy concentration and stress must in fact have played a role in the measured diffusivity. Literature data regarding the role of viscoplastic deformation on diffusivity in Ni–base alloys are very limited. Nguejio [8] studied the tracer diffusion of Cr in Ni at 500 °C by tensile creep tests, with stress levels between 50 and 75 MPa and strain rates in the order of 1.4 x 10^{-3} – 1.19 x 10^{-2} h^{-1}. They measured an increase of the diffusivity by a factor of 10, which they attributed to (i) the excess of vacancies which are created during creep, (ii) a fast diffusion along dislocations. If we refer to their data, the ratio of the diffusion coefficients with and without stress does not depend linearly on the creep strain rate as described by Buffington and Cohen [22], Eq. (13). Furthermore, the variation of the diffusion coefficient with stress observed by Nguejio et al. [8] is larger than the effect observed in the present experiments. Once again, the experiments of Ref. [8] involve dislocation creep, while the present experiments involve diffusion creep. These results would then suggest that dislocation creep has a larger effect on diffusion than diffusion creep. However, it would be useful to compare the two creep mechanisms for the same material to verify this observation.

Finally, it is useful to put the present results in perspective by considering the typical dispersion observed in diffusion data measured in different laboratories. Campbell and Rukhin studied different estimations of Ni diffusion coefficients

available in the literature and determined an associated uncertainty [23]. They have shown that at high temperature (977–1394 °C), once the literature data have been filtered to retain only the most reliable datasets, one can still observe a difference of a factor of ten between diffusion coefficients at one given temperature. This is much greater than the variation due to the effect of external stress observed in the present study.

5 Conclusion

This work illustrates the influence of moderate compressive uniaxial load and of hydrostatic pressure on the interdiffusion coefficient. In the NiCr and NiSi systems, a small decrease of the diffusion coefficient with compressive hydrostatic stress at 1200 °C is observed. However, the variation is very low, even at 326 MPa. This result is consistent with previous studies, which show that the effect of elastic stress becomes significant at much higher pressures. This work also highlights the lack of any visible influence of the viscoplastic deformation during a uniaxial compression creep test on the interdiffusion coefficient in the NiCr system.

To conclude, our results indicate that a very high stress value is needed to see a significant effect on diffusion in Ni–base alloys at high temperature. In this work, the diffusion coefficient is at most multiplied by 1.7, which is smaller than the experimental dispersion typically observed between different laboratories in high temperature diffusion studies. Therefore, the selection of the diffusion data for a simulation is more important than the consideration of the effect of stress on diffusivity. For example, for structural Ni–based alloys used for turbine blades subjected locally to stress values up to 300 MPa, the effect of a uniform uniaxial or hydrostatic stress on the diffusion coefficient values is likely to be not significant and does not necessarily have to be taken into account in lifetime modelling.

6 Acknowledgements

The authors would like to thank C. Lopes (ONERA) for producing the ingots, D. Mézières (ONERA), C. Liard (ONERA) for conducting the creep and compression, respectively, as well as C. Rio (ONERA), N. Horezan (ONERA) and D. Boivin (ONERA) for help with SEM analysis. The HIP experiments were conducted at the CARAMEL platform of the Laboratoire de Sciences des Procédés et des Matériaux, Université Sorbonne Paris Nord, by A. Hocini, who is gratefully acknowledged. We would also like to thank members of the COnCOrD GdR (CNRS, GdR 2081), as this work benefited from fruitful discussions at meetings of the GdR. This work was funded in part by the Agence Nationale de la Recherche (France), grant number ANR-19-CE08-0004.

7 Conflict of interest

The authors declare that they have no conflict of interest.

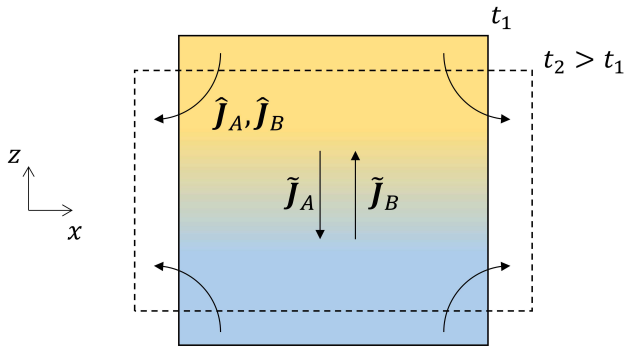

Figure A1: 2D illustration of interdiffusion and convection fluxes in an AB diffusion couple subject to a uniaxial creep test.

Appendix Consideration of the viscoplastic deformation in the determination of interdiffusion coefficients

We consider a diffusion couple made of two AB alloys of different compositions, with the initial interface in the (x, y) plane. The couple is subject to a uniaxial compression creep test, with the load applied along direction z. The problem geometry is represented in 2D in Figure A1, where direction y is omitted for clarity. Creep causes the couple to shrink in the z direction, and to expand in the x and y directions. We assume that the mass transport associated with creep occurs via the bulk motion of the material, i.e., it is a convective form of transport. This implies that in the absence of an initial composition gradient, creep alone would not produce any composition change. This hypothesis neglects fluxes of A and B generated by the vacancy flux when A and B have different mobilities.

We note c_A and C_A the concentration of species A in the laboratory reference frame and in the material reference frame, respectively. The laboratory reference frame is attached to one corner of the sample at the initial state and does not change over time. On the contrary, the material reference frame is attached to one corner of the sample, which moves with time (in the laboratory reference frame), and strains along with the sample. The material derivative, noted $\dot{C}_\mathrm{A}$, is defined as:

$$\dot{C}_\mathrm{A} = \frac{\partial c_\mathrm{A}}{\partial t} + \boldsymbol{v} \cdot \mathrm{grad}\ c_\mathrm{A} \tag{A1}$$

where v is the material velocity field. In Eq. (A1) and in the following, bold letters indicate vector quantities.

In the laboratory frame of reference, the continuity equation for A reads:

$$\frac{\partial c_\mathrm{A}}{\partial t} = -\mathrm{div}\ \boldsymbol{J}_\mathrm{A} \tag{A2}$$

where $\boldsymbol{J}_\mathrm{A}$ is the 3D flux of A, which contains two contributions, the interdiffusion flux $\tilde{\boldsymbol{J}}_\mathrm{A}$ and the convection flux due to creep $\hat{\boldsymbol{J}}_\mathrm{A}$:

$$\boldsymbol{J}_\mathrm{A} = \tilde{\boldsymbol{J}}_\mathrm{A} + \hat{\boldsymbol{J}}_\mathrm{A} \tag{A3}$$

$$\tilde{\boldsymbol{J}}_\mathrm{A} = -\tilde{D} \cdot \mathrm{grad}\ c_\mathrm{A} \tag{A4}$$

$$\hat{\boldsymbol{J}}_{\mathrm{A}} = c_{\mathrm{A}} \cdot \boldsymbol{v} \tag{A5}$$

Substituting Eq. (A3) in Eq. (A2) yields:

$$\frac{\partial c_{\mathrm{A}}}{\partial t} = -\mathrm{div}\ \tilde{\boldsymbol{J}}_{\mathrm{A}} - c_{\mathrm{A}} \cdot \mathrm{div}\ \boldsymbol{v} - \boldsymbol{v} \cdot \mathrm{grad}\ c_{\mathrm{A}} \tag{A6}$$

Combining Eqs. (A1) and (A6) yields:

$$\dot{C}_{\mathrm{A}} = -\mathrm{div}\ \tilde{\boldsymbol{J}}_{\mathrm{A}} - c_{\mathrm{A}} \cdot \mathrm{div}\ \boldsymbol{v} \tag{A7}$$

In continuum mechanics, the divergence of the convective velocity field is defined as the relative volume variation rate:

$$\mathrm{div}\ \boldsymbol{v} = \frac{\dot{V}}{V} \tag{A8}$$

where V is the volume of a representative element of material, typically of the order of a $\mu\mathrm{m}^3$. We make the hypothesis that during creep, the total volume of material is conserved, i.e., we neglect the elastic deformation. Further, we assume that the diffusivity and mechanical properties are uniform throughout the couple. In particular, the convection associated with creep is unaffected by microstructural features such as grain boundaries. It follows that the volume is conserved at the scale of the representative element. This yields $\mathrm{div}\ \boldsymbol{v} = 0$ by virtue of Eq. (A8). Equation (A7) then reads:

$$\dot{C}_{\mathrm{A}} = -\mathrm{div}\ \tilde{\boldsymbol{J}}_{\mathrm{A}} \tag{A9}$$

Equation (A9) is a continuity equation in the material reference frame. It expresses the fact that in the case of a constant-volume transformation, the mass balance defined in the deforming material is directly obtained from the divergence of the interdiffusion flux.

Finally, with the hypothesis of uniform material properties, the initial symmetry of the problem is conserved throughout the transformation. It follows that the x and y coordinates of $\tilde{\boldsymbol{J}}_{\mathrm{A}}$ are 0. Equation (A9) then reduces to a 1D equation:

$$\dot{C}_{\mathrm{A}} = \frac{\partial}{\partial z}\left(\tilde{D}_{\mathrm{AB}} \frac{\partial c_{\mathrm{A}}}{\partial z}\right) \tag{A10}$$

Numerically, this equation is solved by the finite difference method, where the deformation is taken into account by updating the grid size Δz at each time step, as illustrated in Figure 6.

References

[1] D.Y. Li and L.Q. Chen: *Scr. Mater.*, 1997, vol. 37, pp. 1271–7.
[2] L.A. Girifalco and H.H. Grimes: *The Theory of Diffusion in Strained Systems*, NASA, 1959.
[3] D.L. Beke: *Defect Diffus. Forum*, 1996, vol. 129–130, pp. 9–30.
[4] H. Mehrer: *Defect Diffus. Forum*, 2011, vol. 309–310, pp. 91–112.
[5] R. Nakamura, K. Fujita, Y. Iijima, and M. Okada: *Acta Mater.*, 2003, vol. 51,

pp. 3861–70.
[6] J.-W. Jang, J. Kwon, and B.-J. Lee: *Scr. Mater.*, 2010, vol. 63, pp. 39–42
[7] D. Connétable and P. Maugis: *Acta Mater.*, 2020, vol. 200, pp. 869–82.
[8] J. Nguejio Nguimatsia: thesis, Paris Sciences et Lettres, 2016.
[9] T. Gheno, F. Jomard, C. Desgranges, and L. Martinelli: *Materialia*, 2018, vol. 3, pp. 145–52.
[10] S.K. Kailasam, J.C. Lacombe, and M.E. Glicksman: *Metall. Mater. Trans. A*, 1999, vol. 30, pp. 2605–10.
[11] R. Bouchet and R. Mevrel: *Acta Mater.*, 2002, vol. 50, pp. 4887–900.
[12] J. Philibert: *Diffusion et transport de matière dans les solides*, les éditions de physique, Les Ulis, France, 1985.
[13] SciPy v1.8 Manual, https://docs.scipy.org/doc/scipy/reference/odr.html, (accessed 15 February 2022).
[14] NumPy v1.22 Manual, https://numpy.org/doc/stable/reference/, (accessed 17 February 2022).
[15] J.C. Schuster and Y. Du: *Metall. Mater. Trans. A*, 2000, vol. 31, pp. 1795–803
[16] Y. Du and J.C. Schuster: *Z. Fuer Met. Res. Adv. Tech.*, 2001, vol. 92, pp. 28–31.
[17] M.A. Dayananda: *Metall. Trans. A*, 1983, vol. 14, pp. 1851–8.
[18] B. Jönsson: *Scand. J. Metall.*, 1995, vol. 24, pp. 21–7.
[19] B.-J. Lee: *Calphad*, 1992, vol. 16, pp. 121–49.
[20] A.J. Ardell and S.V. Prikhodko: *Acta Mater.*, 2003, vol. 51, pp. 5013–9
[21] M.J. Aziz, Y. Zhao, H.-J. Gossmann, S. Mitha, S.P. Smith, and D. Schiferl: *Phys. Rev. B.*
[22] F.S. Buffington and M. Cohen: *JOM*, 1952, vol. 4, pp. 859–60.
[23] C.E. Campbell and A.L. Rukhin: *Acta Mater.*, 2011, vol. 59, pp. 5194–201.